

# Synthesis and Characterization of a New Soluble, Structurally Well-Defined Conjugated Polymer Alternating Regioregularly Alkylated Thiophene Oligomer and 2,2'-Bipyridine Units: Metal-Free Form and Ru(II) Complex

L. Trouillet, A. De Nicola, and S. Guillerez\*

Département de Recherche Fondamentale sur la Matière Condensée, SI3M/EMSI, CEA Grenoble, 17, rue des Martyrs, 38054 Grenoble Cedex 09, France

Received December 28, 1999. Revised Manuscript Received April 5, 2000

The Pd-catalyzed Stille cross-coupling reaction has been used to synthesize novel  $\pi$ -conjugated polymers based on regioregular 3-(octylthiophene) tetramers alternated with either 2,2'-bipyridine or its Ru(II) complex ( $\text{Ru}(\text{bipy})_3^{2+}$ ). A preliminary optimization of the cross-coupling conditions enabled the synthesis of high molecular, structurally defined, and defect-free copolymers. Both are well-soluble in common organic solvents, which allowed their easy characterization by standard  $^1\text{H}$  NMR and UV–visible spectroscopies as well as by electrochemical techniques. Interestingly,  $^1\text{H}$  NMR spectra not only confirmed the structure of the synthesized polymers but also contributed to estimating the length of polymer chains together with gel permeation chromatography and light-scattering experiments. UV–visible experiments indicated that the delocalization of  $\pi$ -orbitals occurs efficiently in our conjugated structures and involves both oligothiophene and metal-free or ruthenium chelating bipyridine units, while electrochemical experiments revealed electronic interactions between the conjugated backbone and the ruthenium complexes in the metal-containing polymer.

## Introduction

Conducting polymers constitute an important class of organic materials, which are extensively studied due to their remarkable optical and electronic properties in both their neutral and oxidized states.<sup>1</sup> In the past few years, tremendous progress in the design, synthesis, and processability was accomplished leading to materials with enhanced properties compatible with applications such as LED's or organic transistors. In addition to this major field of research, which corresponds to a "material approach", increasing efforts were devoted to the design of multicomponent  $\pi$ -conjugated polymers whose properties should be controlled at a molecular level.<sup>2–11</sup> This has led to a few reported syntheses of metal-containing

conjugated polymers in which the metal center and the conjugated backbone are in strong interaction such that a stimulus properly applied to one of the components will significantly modify the properties of the other one.<sup>12–23</sup> Then, depending on the intrinsic properties of the interacting moieties, the resulting multicomponent  $\pi$ -conjugated polymer should in principle exhibit new tunable electrochemical, photophysical, magnetic, or transport properties associated with an array of potential uses (e.g., electrocatalysis, molecular recognition, photoconductivity, and molecular electronics). In all these systems, the metallic core is affixed to the

(1) See, for example: Skotheim, T. A.; Elsenbaumer, R. L.; Reynolds, J. R. *Handbook of conducting polymers*, 2nd ed; Marcel Dekker: New York, 1998. Proceedings of ICSM 1998 *Synth. Met.* **1999**, 101–103.

(2) Segawa, H.; Hakayama, N.; Wu, F.; Shimidzu, T. *Synth. Met.* **1993**, 55–57, 966.

(3) McCullough, R. D.; Williams, S. P.; Jayaraman, M. *Polym. Prepr.* **1994**, 35, 190.

(4) Miyazaki, Y.; Kanbara, T.; Osaka, K.; Yamamoto, T.; Kubota, K. *Polym. J.* **1994**, 26, 509.

(5) Yamamoto, T.; Kizu, K.; Maruyama, T.; Ooba, N.; Tomaru, S.; Kubota, K. *Chem. Lett.* **1994**, 913.

(6) Marsella, M. J.; Newland, R. J.; Carroll, P. J.; Swager, T. M. *J. Am. Chem. Soc.* **1995**, 117, 9842.

(7) Marsella, J. M.; Carroll, P. J.; Swager, T. M. *J. Am. Chem. Soc.* **1995**, 117, 9832.

(8) Shimidzu, T.; Segawa, H.; Wu, F.; Nakayama, N. *J. Photochem. Photobiol. A: Chem.* **1995**, 92, 121.

(9) Yamamoto, T.; Zhou, Z.-h.; Kanbara, T.; Shimura, M.; Kizu, K.; Maruyama, T.; Nakamura, Y.; Fukuda, T.; Lee, B.-L.; Ooba, N.; Tomaru, S.; Kurihara, T.; Kaino, T.; Kubota, K.; Sasaki, S. *J. Am. Chem. Soc.* **1996**, 118, 10389.

(10) McCullough, R. D.; Ewbank, P. C.; Loewe, R. S. *J. Am. Chem. Soc.* **1997**, 119, 633.

(11) Yun, H.; Kwei, T. K.; Okamoto, Y. *Macromolecules* **1997**, 30, 4633.

(12) Funaki, H.; Aramaki, K.; Nishiara, H. *Chem. Lett.* **1992**, 2065.

(13) Yamamoto, T.; Maruyama, T.; Zhou, Z.; Ito, T.; Fukuda, T.; Yoneda, Y.; Begum, F.; Ikeda, T.; Sasaki, S.; Takezoe, H.; Fukuda, A.; Kubota, K. *J. Am. Chem. Soc.* **1994**, 116, 4832. Maruyama, T.; Yamamoto, T. *Inorg. Chim. Acta* **1995**, 238, 9.

(14) Wolf, O.; Wrighton, M. S. *Chem. Mater.* **1994**, 6, 1526.

(15) Zhu, S. S.; Swager, T. M. *Adv. Mater.* **1996**, 8, 497. Zhu, S. S.; Swager, T. M. *J. Am. Chem. Soc.* **1997**, 119, 12568.

(16) Cameron, C. G.; Pickup, P. G. *Chem. Commun.* **1997**, 303.

(17) Ley, K. D.; Whittle, C. E.; Bartkerger, M. D.; Schanze, K. S. *J. Am. Chem. Soc.* **1997**, 119, 3423. Ley, K. D.; Schanze, K. S. *Coord. Chem. Rev.* **1998**, 171, 287.

(18) Wang, B.; Wasielewski, M. R. *J. Am. Chem. Soc.* **1997**, 119, 12.

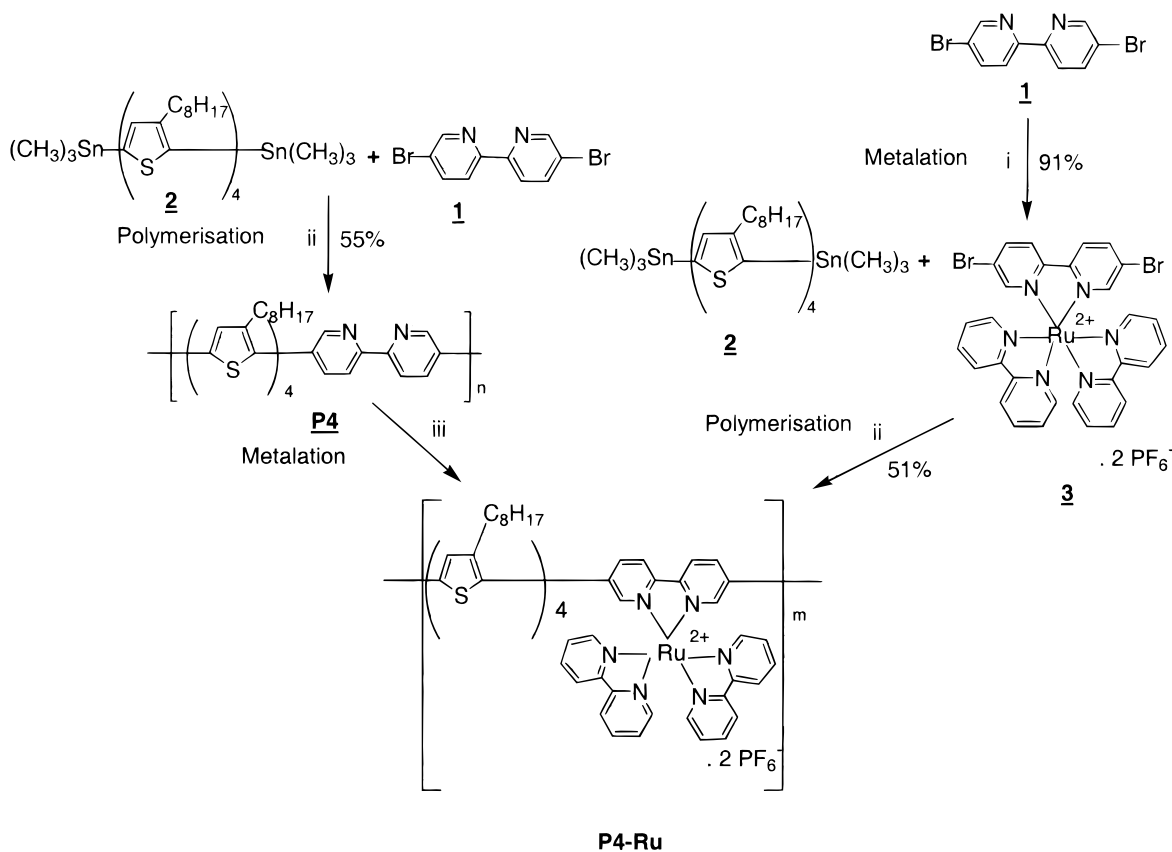
(19) Peng, Z.; Gharavi, A. R.; Yu, L. *J. Am. Chem. Soc.* **1997**, 119, 4622–4632. Wang, Q.; Wang, L.; Yu, L. *J. Am. Chem. Soc.* **1998**, 120, 12860.

(20) Vidal, P. L.; Billon, M.; Divisia-Blohorn, B.; Bidan, G.; Kern, J. M.; Sauvage, J. P. *Chem. Commun.* **1998**, 629.

(21) Reddinger, J. L.; Reynolds, J. R. *Chem. Mater.* **1998**, 10, 1236–1243. Reddinger, J. L.; Reynolds, J. R. *Chem. Mater.* **1998**, 10, 3.

(22) Yu, S. C.; Gong, X.; Chan, W. K. *Macromolecules* **1998**, 31, 5639.

(23) Plenio, H.; Herman, J.; Leukel, J. *Eur. J. Inorg. Chem.* **1998**, 2063.

Scheme 1<sup>a</sup>

<sup>a</sup> Conditions: (i) Ru(bipy)<sub>2</sub>Cl<sub>2</sub>, ethanol 96% reflux; (ii) Pd(PPh<sub>3</sub>)<sub>2</sub>, DMF, 120 °C; (iii) efficient conditions have not been found until now.

conjugated polymer backbone by bidentate heterocyclic diimine moieties. The type of structures thus obtained associates some fundamental advantages. On the one hand, the bidentate ligand unit can be included into the conjugated backbone without any formal conjugation disruption, which should therefore lead to strongly coupled structures. On the other hand, the diimine ligands enable the complexation of numerous transition metals, forming coordination compounds with recognized redox, photophysical, and magnetic properties.<sup>24</sup>

Our group has recently reported on the first efficient regiospecific synthesis of head-to-tail coupled oligo(3-alkylthiophenes).<sup>25</sup> These oligomers are the molecules of choice to build such multicomponent  $\pi$ -conjugated polymers. Introduction of reacting groups at the terminal positions  $\alpha$  to sulfur can be easily achieved and allows a subsequent reaction with a second bis-functionalized ligand molecule leading to a polymer. By the use of an appropriate coupling reaction, a defect-free conjugated structure with alternating thiophene oligomer and ligand moieties could then be obtained. Two other main advantages guided our choice: (1) Due to the grafting of an alkyl chain on each thiophene ring, the incorporation of such oligomers will help to solubilize the final polymer. This is a critical point with regard to its chemical structure characterization, its study both in solution and in the film state, and its further metalation. (2) Within this series of oligo(3-alkylthio-

phenes), redox and photophysical properties are varying depending on the length of the oligomer, so that a homogeneous family of polymers with reliable structure/property relationship will be accessible.<sup>25,26</sup>

In a classical way, we selected 2,2'-bipyridine (bipy) as the complexing unit to be incorporated between oligothiophene moieties to form polymers. In addition to its usual complexation properties, the bipy moiety offers other options that must be pointed out. The polymer ligand (metal-free), constituted by a regular alternation of electron-rich (oligothiophene) and electron-poor (bipyridine) units, may exhibit interesting transport properties as previously mentioned by Yamamoto and co-workers.<sup>9</sup> Moreover, new materials with different electronic properties will be accessible by either alkylation (to give diquat analogues) or reversible protonation.<sup>11</sup>

Therein we report on the syntheses of the metal-free polymer **P4** based on the alternation of the regioregular octylthiophene tetramer with 2,2'-bipyridine and of the corresponding ruthenium(II) complex **P4-Ru**, with their characterizations by electrochemistry and UV-vis and <sup>1</sup>H NMR spectroscopies.

## Results and Discussion

As shown in Scheme 1, two synthetic ways have been investigated. In the first one, the conjugated polymer backbone is constructed prior to the metalation step,

(24) Constable, E. C. *Adv. Inorg. Chem.* **1989**, *34*, 1.

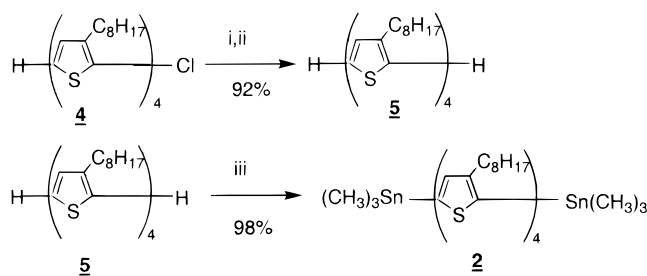
(25) Bidan, G.; De Nicola, A.; Enée, V.; Guillerez, S. *Chem. Mater.* **1998**, *10*, 1052.

(26) Barth, M.; Lapkowski, M.; Bidan, G.; Guillerez, S. Results to be published.

which give access to the metal-free polymer **P4**; the latter can then be metalated by an appropriate ruthenium precursor to give **P4–Ru**. This approach will furthermore allow changing the nature of the introduced transition metal to give a series of metal-containing polymers. In the second one, the heteroleptic metallic core bearing one bis-functionalized bipy is synthesized first, and then polymerized leading to **P4–Ru**. This will lead to a polymer in which every bipy is metalated, whereas the metal amount in the polymer obtained with the first strategy will very probably remain uncertain. The drawback, with this strategy consisting in the heterocoupling of two bifunctional units, one symmetrical and not the other one, is that the whole polymer will not be regioregular. In fact, three differently substituted bipyridine units will be present in the polymeric structure: (a) some bipyridines coupled with two sterically hindered sides (two heads) of oligothiophenes, (b) some bipyridines coupled with two free sides (two tails) of oligothiophenes, and (c) some bipyridines coupled with two different sides (one head and one tail) of oligothiophenes.

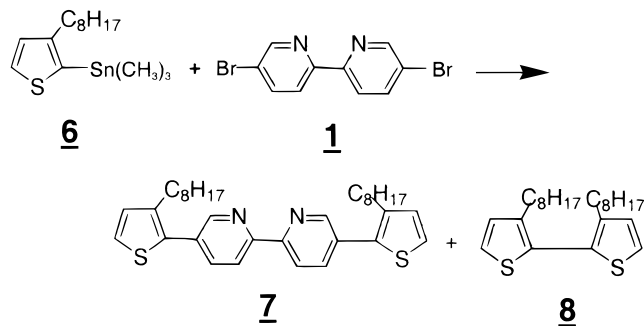
**Synthesis.** For both options, the crucial step is constituted by the coupling reaction between oligothiophene and bipyridine moieties and a particular attention was pointed in that direction. Although the Suzuki coupling was found by us<sup>25</sup> and others<sup>27,28,29</sup> to be extremely efficient in the synthesis of thiophene-based oligomers, its application to polymer synthesis is problematic because of the instability of the 2-thienylboronic acid derivatives toward coupling conditions.<sup>25,27,30</sup> In contrast, the Stille coupling reaction, which does not seem to suffer from such inconvenience<sup>31</sup> and was used with success in the thiophene series<sup>28,32,33</sup> appeared well-adapted to our purposes. Therefore, our polymers were constructed from bis-stannylated quaterthiophene and 5,5'-dibromo-2,2'-bipyridine units.

**Synthesis of the Precursors.** The chlorinated regioregular quater(3-octylthiophene) **4** was synthesized according to a procedure recently published by us,<sup>25</sup> and the radical reduction using tributyltin hydride in the presence of  $\alpha,\alpha'$ -azoisobutyronitrile (AIBN) produced the free-ends oligomer **5** (Scheme 2). Compared to our previous work, the yield of the dechlorination reaction was significantly increased (from 70% to 92%) by simply treating the crude product with *p*-toluenesulfonic acid. In fact, in addition to the major free-ends quaterthiophene, the radical reaction produced about 20% of a stannylated derivative (detected by reverse-phase HPLC) by substitution of the chlorine with tributylstannyl, instead of proton. The acidic workup allowed the total conversion of this byproduct into **5**. The bis-trimethyltin derivative **2** was then obtained by lithiation and quenching of the dianion of **5** with trimethyltin chloride. The stability of the organometallic reagent enabled an HPLC reverse-phase analysis of the crude

Scheme 2<sup>a</sup>

<sup>a</sup> Conditions: (i) Bu<sub>3</sub>SnH, AIBN, THF; (ii) *p*-toluenesulfonic Acid; (iii) 2.5 equiv of *n*-BuLi, Me<sub>3</sub>SnCl.

Scheme 3



product, which was shown to contain 98.3% of the desired bis-stannylated compound and 1.7% only of the mono-stannylated derivatives. Compound **2** was finally obtained with a yield of 98% and a purity of 99.5% by semipreparative reverse-phase HPLC. The 5,5'-dibromo-2,2'-bipyridine **1** was synthesized according to a procedure described by Romero et al.<sup>34</sup> Its reaction with Ru(bipy)<sub>2</sub>Cl<sub>2</sub><sup>35</sup> in ethanol 96% under reflux was monitored by UV–visible spectroscopy in ethanol. The disappearance of the band at 534 nm, characteristic of the MLCT absorption of Ru(bipy)<sub>2</sub>Cl<sub>2</sub>,<sup>36</sup> and the increase of the band at 447 nm, characteristic of the MLCT absorption of Ru(bipy)<sub>3</sub><sup>2+</sup>,<sup>37</sup> indicated the formation of the complex **3**.

**Optimization of the Cross-Coupling Reaction.** The length of polymers **P4** and **P4–Ru** will depend on the yield of the cross-coupling reaction (the higher the yield, the longer the polymer), and it is thus necessary to find the best adapted conditions to perform the Stille reaction. Particular attention will be directed toward the homocoupling reaction of the tin reagent<sup>31</sup> which in our case will lead to irregularities in the polymer structure by doubling the length of the oligothiophene moiety, and will cause a stoichiometric imbalance of the reactants.

This led us to study the reaction between the 5,5'-dibromo-2,2'-bipyridine **1** and the sterically hindered 2-trialkylstannyl-3-octylthiophene **6** (Scheme 3). In fact, the Stille reaction with heteroarylstannanes is known to be very sensitive to steric hindrance: an alkyl group in ortho position to the tin residue can decrease the coupling rate by a factor of ~20.<sup>31</sup> Obtaining a good yield

(27) Gronowitz, S.; Peters, D. *Heterocycles* **1990**, *30*, 845.

(28) Tour, J. M.; Wu, R. *Macromolecules* **1992**, *25*, 1901.

(29) Kirschbaum, T.; Azumi, R.; Mena-Osteritz, E.; Bauerle, P. *New J. Chem.* **1999**, 241.

(30) Guillerez, S.; Bidan, G. *Synth. Met.* **1998**, *93*, 123.

(31) Farina, V.; Krishnamurthy, V.; Scott, W. J. *Org. React.* **1997**, *50*, 1–61.

(32) Wei, Y.; Yang, Y.; Yeh, J. M. *Chem. Mater.* **1996**, *8*, 2659.

(33) Antolini, L.; Goldoni, F.; Iarossi, D.; Mucci, A.; Schenetti, L. *J. Chem. Soc., Perkin Trans. 1* **1997**, 1957.

(34) Romero, F. M.; Ziesel, R. *Tetrahedron Lett.* **1995**, *36*, 6471.

(35) Sullivan, B. P.; Salmon, D. J.; Meyer, T. J. *Inorg. Chem.* **1978**, *17*, 3334.

(36) Fergusson, J. E.; Harris, G. M. *J. Chem. Soc. (A)* **1966**, 1293.

(37) Juris, A.; Balzani, V.; Barigelletti, F.; Campagna, S.; Belser, P.; Von Zelewsky, A. *Coord. Chem. Rev.* **1988**, *84*, 85.

**Table 1. Results Obtained during the Study of the Cross-Coupling Reaction between the 5,5'-Dibromo-2,2'-bipyridine **1** and the Sterically Hindered 2-Trialkylstannyl-3-octylthiophene **6** (see Scheme 3)**

entry	coupling conditions				results	
	solvent	<i>T</i> (°C)	catalyst	reaction time <sup>a</sup>	yield of <b>7</b> , %	<b>8/7</b> , <sup>b</sup> %
a	DMF	120	Pd(PPh <sub>3</sub> ) <sub>3</sub>	16 h	71	<i>c</i>
b	DMF	120	Pd(AsPh <sub>3</sub> ) <sub>4</sub>	3 d	40	1
c	DMF	120	Pd(dppf)Cl <sub>2</sub>	2 d	50	2
d	DMF	120	Pd(PPh <sub>3</sub> ) <sub>2</sub> Cl <sub>2</sub>	16 h	88	8
e	DMF	120	Pd(PPh <sub>3</sub> ) <sub>2</sub>	16 h	88	0.3
f	toluene	110	Pd(PPh <sub>3</sub> ) <sub>3</sub>	7 d	47	7
g	pyridine	130	Pd(PPh <sub>3</sub> ) <sub>2</sub>	24 h	83	3

<sup>a</sup> Time after which the reaction ended spontaneously. <sup>b</sup> Established from the results of HPLC reverse phase analysis. <sup>c</sup> Not determined.

with an analogue of the least reactive position of the thiophene oligomer will guarantee an excellent yield for the polymerization reaction. Several criteria have been checked successively: the nature of the catalyst and the solvent, the reaction time and the catalyst amount. All the test reactions were carried out in a similar way: (1) the reaction mixtures were always carefully degassed by multiple freeze–thaw–pump cycles because atmospheric oxygen is known to promote homocoupling of the tin reagents; (2) the tin reagent was used in a moderate excess of 10% (2.2 equiv versus 5,5'-dibromo-2,2'-bipyridine); (3) all reactions were carried out under an argon atmosphere and were monitored by reverse-phase HPLC. The results are summarized in Table 1. The role of the catalyst was examined by performing the test reaction in DMF at 120 °C with a fixed amount of various palladium catalysts (0.06 equiv versus 5,5'-dibromo-2,2'-bipyridine). With the commonly used tris(triphenylphosphine) palladium(0) (Pd(PPh<sub>3</sub>)<sub>3</sub>, entry a), the reaction proceeded rapidly but produced only a moderate yield of the final disubstituted bipyridine **7**. The use of ligands with reduced donicity such as triphenylarsine (AsPh<sub>3</sub>; entry b), known to accelerate the rate-limiting transmetalation step,<sup>31</sup> or with strong chelating ability such as 1,1'-bis(diphenylphosphinoferrocene) (dppf; entry c), known to stabilize catalytic species, lowered dramatically the yield of the coupling reaction below 50%. Coming back with triphenylphosphine, the more coordinatively unsaturated catalysts Pd(PPh<sub>3</sub>)<sub>2</sub>Cl<sub>2</sub> (entry d) and Pd(PPh<sub>3</sub>)<sub>2</sub><sup>39</sup> (entry e) (generally, the turnover rate increases when the number of triphenylphosphine ligands decreases, with the counterpart of a lower thermal stability<sup>38</sup>) gave isolated yields of **7** up to 88%. In both cases, analyses of the crude products showed the complete consumption of the starting 5,5'-dibromo-2,2'-bipyridine and only traces of the intermediate monosubstituted product. In the case of the stable, commercially available Pd(PPh<sub>3</sub>)<sub>2</sub>Cl<sub>2</sub>, the higher ratio in homocoupled byproduct **8** was expected because of the necessary reduction of this precursor to form the active Pd(0) catalyst, which is often achieved through the homocoupling of 2 equiv of stannane.<sup>31</sup> Then, we have been interested in the choice of a solvent, which is a factor affecting not only the coupling ef-

iciency but also the solubility of the polymer in the reaction medium and then the polymer molecular weight. The use of solvents of lower polarity (toluene and pyridine, entries f and g respectively) that could better solubilize the apolar unmetalated polymer **P4** gave unsatisfactory results with the best catalyst previously determined (poor yield for toluene and high amount of homocoupled byproduct for pyridine). Although very few solvents have been tested, DMF appeared to be the appropriate solvent for the polymerization reactions, particularly for the synthesis of the polar **P4–Ru**. A final test reaction was carried out to determine the amount of catalyst and the reaction time necessary to complete the polymerization reaction. The best predetermined conditions (Pd(PPh<sub>3</sub>)<sub>2</sub>, DMF, 120 °C) were used with an amount of 0.006 equiv of catalyst versus 5,5'-dibromo-2,2'-bipyridine, which was known to be too small to go to completion. The progress of the reaction was monitored by reverse-phase HPLC. It was shown that (1) the reaction started rapidly with an initial conversion rate of 30%/h (estimated on the first 15 min), but the rate decreased rapidly and a conversion factor of 40% was observed after 6 h. (2) The reaction ended spontaneously after 20 h of heating, very probably due to thermal decomposition of the catalyst, and a conversion factor of 0.5 (corresponding to a turnover of about 167) was observed. (3) Further addition of catalyst was inefficient to restart the reaction, whereas both reactants were still present in the reaction mixture. Thus, the catalyst must be introduced at the beginning of the reaction in sufficient quantity to go to completion. Accordingly, we decided to carry out the polymerization using 3% equiv versus 5,5'-dibromo-2,2'-bipyridine of Pd(PPh<sub>3</sub>)<sub>2</sub> and a reaction time of 24 h. With these conditions, the test reaction gave the bis-substituted bipyridine **7** with a yield of 91% after chromatography (the small increase of the yield compared to entry e of Table 1 was not significant enough to be attributed to the longer reaction time). In a similar way, we performed the coupling reaction between the same tin reagent **6** and the dibrominated ruthenium(II) complex **3** (Scheme 4). After 6 h of heating, the starting complex had been entirely consumed, and the bis-functionalized complex **9** was isolated with 98%, showing that the Stille coupling reaction may be applied with success to both synthetic options described in Scheme 1.

**Synthesis of Polymers **P4** and **P4–Ru**.** For the synthesis of polymers **P4** and **P4–Ru**, strictly equivalent amounts of bis-stannylated quaterthiophene **2** and dibrominated precursors (respectively 5,5'-dibromo-2,2'-bipyridine **1** and the dibrominated ruthenium complex **3**) were allowed to react in the coupling conditions determined above (Pd(PPh<sub>3</sub>)<sub>2</sub>, DMF, 120 °C/24 h, absence of oxygen). The unmetalated polymer **P4** was insoluble in the reaction mixture and precipitated as it was formed, whereas the metalated **P4–Ru** remained soluble. The crude polymer **P4** was easily collected and purified in a Soxhlet apparatus by successive extractions with ethanol, *n*-hexane, and 1,2-dimethoxyethane (DME). Finally, the resulting solid was extracted with boiling chloroform to give 55% of **P4** as the soluble part, and 6.5% of an insoluble polymer. Analysis of the different fractions by gel permeation chromatography (GPC) shows that the shorter oligomers were efficiently re-

(38) Farina, V.; Krishnan, B. *J. Am. Chem. Soc.* **1991**, *113*, 9585.

(39) Negishi, E.; Takahashi, T.; Akiyoshi, K. *J. Chem. Soc., Chem. Commun.* **1986**, 1338.

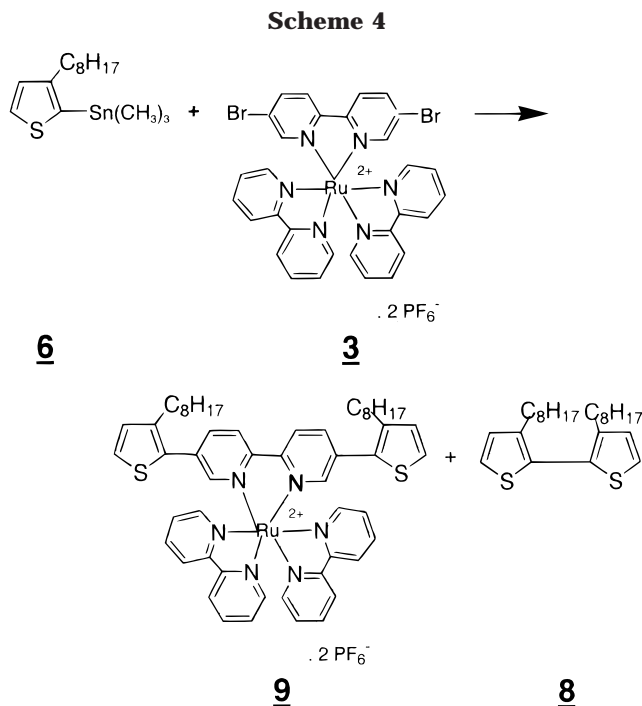


**Table 2. GPC Determined Molecular Weights and Relative Quantities of the Fractions Collected during the Purification of Polymer P4**

	solvent	$M_n$	$M_w$	yield, %
part 1	ethanol	3 300	4 400	4
part 2	hexane	4 700	5 600	10
part 3	dme	11 000	16 000	14
part 4	chloroform	111 000	244 000	55
part 5	insoluble part	?	?	6.5

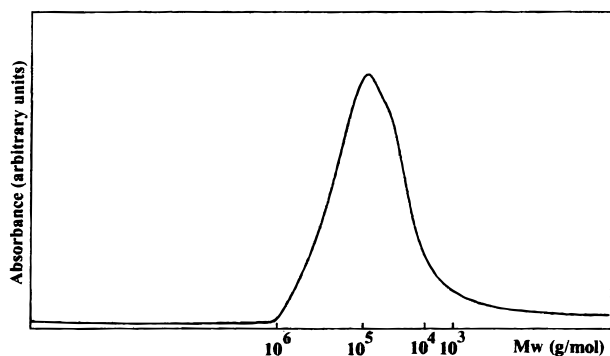


**Figure 1.** Molecular weight distribution of polymer **P4** as determined by GPC.

moved, leading to a polymer with a relatively high molecular weight in number  $M_n = 111\,000\text{ g mol}^{-1}$  (Table 2 and Figure 1). However, it should be pointed out that the molecular weights were determined using polystyrenes as standards, which very probably led to overestimate the results. To obtain more reliable values, light scattering experiments were performed in chloroform, but in this case the iso-concentration curves of the Zimm plot did not consist in straight lines, thus indicating the presence of aggregates, which conducted to overestimated results too ( $M_w = 1.3 \times 10^6\text{ g mol}^{-1}$ ). The metalated polymer **P4–Ru** was isolated in its hexafluorophosphate form. Impurities and lower molecular weight polymer were removed by successive extractions in a Soxhlet apparatus with methanol and ethanol, and the final polymer was obtained by precipitation from

an acetonitrile/water mixture with a yield of 51%. Analysis of this polymer by GPC was unsuccessful, and the purification process was monitored by  $^1\text{H}$  NMR spectroscopy in acetonitrile- $d_3$ . The progressive simplification of the recorded spectra, reflecting the disappearance of signals due to impurities and short polymeric chains, indicated that the purity and the molecular weight of **P4–Ru** increased in the course of the purification. The molecular weight of the final **P4–Ru** was estimated from light-scattering experiments conducted in dimethyl sulfoxide at  $25\text{ }^\circ\text{C}$ , giving  $M_w = 70\,000\text{ g mol}^{-1}$  (aggregates were detected when using DMF, leading to an overestimated value for  $M_w$ ). Interestingly both polymers were soluble at room temperature in common organic solvents: **P4** exhibited an appreciable solubility up to  $10\text{ mg/mL}$  in chloroform and a limited solubility of about  $1\text{ mg/mL}$  in 1,1,2,2-tetrachloroethane and 1-methyl-2-pyrrolydinone (NMP). **P4–Ru** was very soluble in a lot of organic solvents such as acetonitrile, DMF, NMP, dimethyl sulfoxide (DMSO), and benzonitrile. This particular point must be outlined and constitutes a decisive advantage of these polymers. Indeed, on one hand it allowed their study by standard spectroscopic and electrochemical techniques and on the other hand it will allow the obtaining of good quality films for their further studies in the solid state. The synthesis of **P4–Ru** by metalation of the polymer **P4** with  $\text{Ru}(\text{bipy})_2\text{Cl}_2$  or  $[\text{Ru}(\text{bipy})_2(\text{EtOH})_2](\text{PF}_6)_2^{40}$  was tested in various conditions (solvent and temperature), but unfortunately the results obtained up to now remained unsatisfactory and only the second strategy (metalation–polymerization) led efficiently to **P4–Ru**.

**Characterization.**  $^1\text{H}$  NMR Spectroscopy. Figure 2 shows the  $^1\text{H}$  NMR spectrum of the unmetalated polymer **P4** recorded at  $70\text{ }^\circ\text{C}$  in 1,1,2,2-tetrachloroethane- $d_2$ . Assignments, confirmed by COSY and ROESY experiments, and the integration ratio between the thiophene and the pyridine parts, are consistent with the expected structure. The region of the bipyridine protons is particularly informative and needs to be discussed in more details. Because of the nonsymmetrical structure of the oligothiophene moiety, the junction positions  $\alpha$  to sulfur are electronically and sterically different. This induces a difference in the response of the bipyridine protons in the vicinity of this junction (namely the protons 4, 4', and 6, 6'). The more shielded signals are assigned to the protons 4 and 6 of the ring connected to the more sterically hindered side; the steric hindrance causes an enhancement of the inter-ring twist angle, diminishing the effect of the current cycle on the neighboring pyridine nucleus. This can be applied to the proton a of the oligothiophene moiety, that is deshielded compared to the other protons b, c, and d. Moreover, two points are in favor of a high molecular weight for polymer **P4**, confirming the GPC data: (1) Only very weak signals that may be assigned to polymer ends were detected. (2) The intensity ratio between protons 4 and 4' and between protons 6 and 6' are equal to unity after baseline corrections (it is smaller for protons 4 and 6 in small polymeric chains because of the lower reactivity of the sterically hindered side of the quarter(3-octylthiophene) moiety). More quantitative results were

(40) Santra, B. K.; Menon, M.; Pal, C. K.; Lahiri, G. K. *J. Chem. Soc., Dalton Trans.* **1997**, 1387.

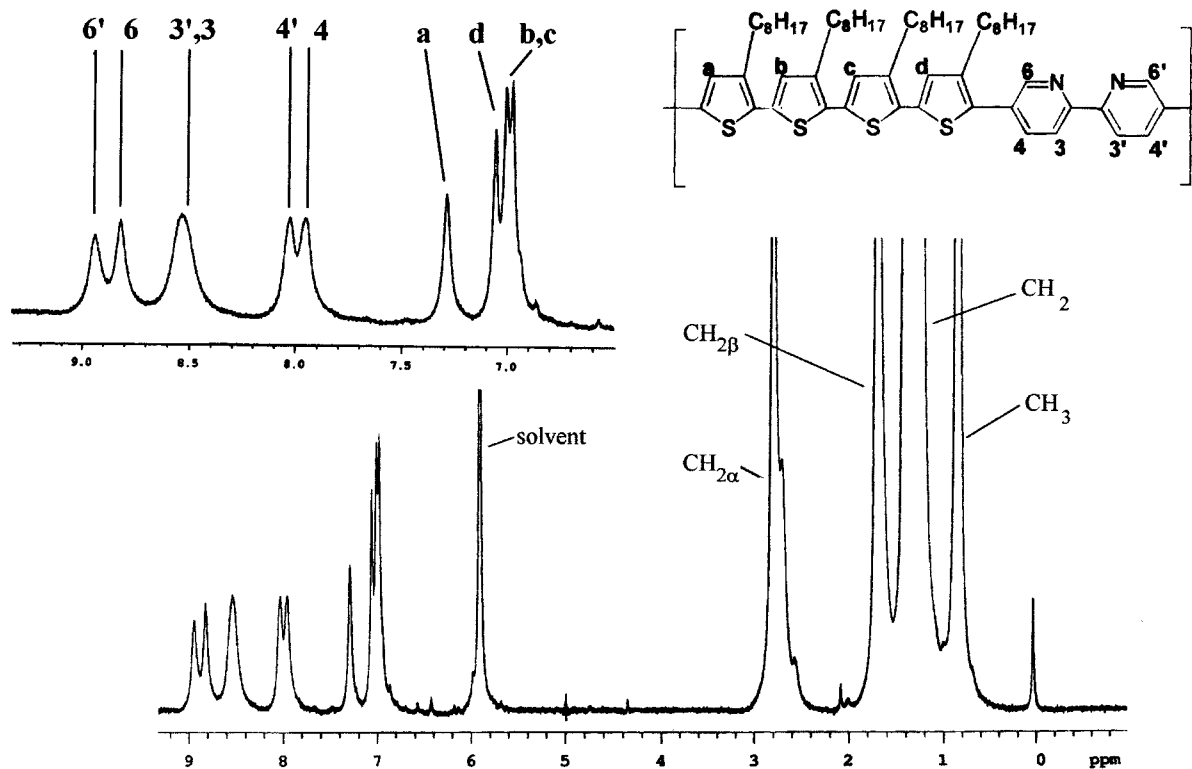


**Figure 2.**  $^1\text{H}$  NMR spectrum (400 MHz) of polymer **P4** in tetrachloroethane- $d_2$  at 343 K.

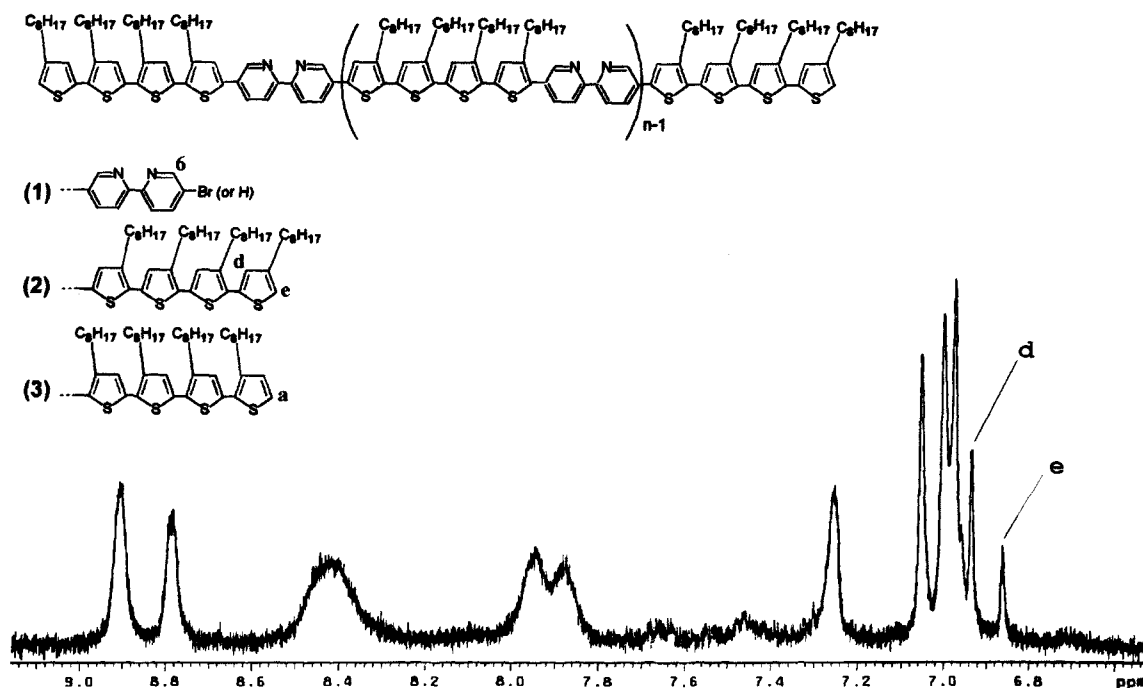


**Figure 3.**  $^1\text{H}$  NMR spectrum (400 MHz) of the lower molecular weight DME extract of polymer **P4** in tetrachloroethane- $d_2$  at 343 K.

obtained by a careful analysis of the spectrum of the lower molecular weight DME extract (Figure 3), which allowed us to determine the nature and abundance of the polymeric chain terminations. Among the protons characteristic of these terminations, only the protons  $\text{H}_d$  and  $\text{H}_e$  associated with the type 2 (respectively at  $\delta = 6.93$  and  $6.86$  ppm) were found to be present in appreciable quantity. The other protons  $\text{H}_6$  and  $\text{H}_a$  characteristic of terminations of the type 1 and 3, which should give signals at  $8.7$  and  $7.1$  ppm,<sup>41</sup> were not detected. We thus considered that the chain ends are

essentially constituted by the hindered side of the quaterthiophene unit as shown by the chemical structure in Figure 3, which is consistent with the lower reactivity of the sterically hindered trimethyltin groups. From this structure and the integration ratio between the bipyridine protons  $\text{H}_6$  and  $\text{H}_{6'}$ , a  $M_w = 6700 \text{ g mol}^{-1}$  was estimated. The integration ratio between the terminal proton  $\text{H}_e$  and the bipyridine protons  $\text{H}_3$  gave a slightly higher value of the molecular weight ( $M_w = 8100 \text{ g mol}^{-1}$ ), which is probably less accurate because of the imprecise determination of the integration value

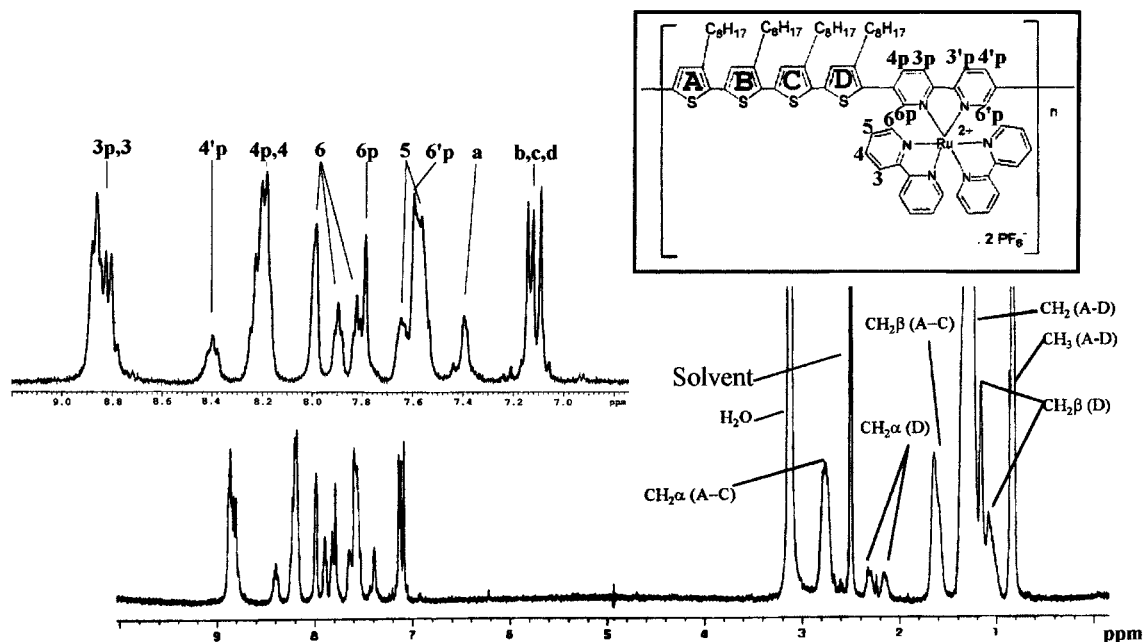


**Figure 4.**  $^1\text{H}$  NMR spectrum (400 MHz) of polymer **P4–Ru** in  $\text{DMSO-}d_6$  at 343 K.

of the low intensity signal of the proton  $\text{H}_e$ . Considering the value of  $M_w = 6700 \text{ g mol}^{-1}$  as being the exact value for the molecular weight, it was then possible to recalibrate the GPC data previously obtained by applying a correcting factor of 0.6. In the NMR spectrum of the polymer **P4**, the only detected termination signature was a very weak singlet at  $\delta = 6.87 \text{ ppm}$  assigned to terminal  $\text{H}_e$  protons. There is then every reason to assume that **P4** is structurally identical to the lower molecular weight polymer fraction, presenting essentially the hindered side of the quaterthiophene unit as chain ends (type 2 in Figure 3). By applying the correcting factor previously determined to the GPC data, we determined a new value for the molecular weight in number,  $M_n = 67\,000 \text{ g mol}^{-1}$ , corresponding to about 70 monomer units.

The  $^1\text{H}$  NMR spectrum of the metalated polymer **P4–Ru** was recorded in dimethyl sulfoxide- $d_6$  at  $70^\circ\text{C}$ , and the assignment was established by comparison with model complexes (**9**) and by the use of 2D techniques (COSY and ROESY). The resulting spectrum is rather complicated because of the absence of symmetry in the polymer as depicted by the chemical drawing of Figure 4, where each pyridine ring is different from the others. In the aliphatic region, the methylene protons of the octyl chain on the thiophene ring D give individually well identified signals. This large upfield shift and the splitting of the signal of the prochiral  $\alpha$  methylene protons indicate that the octyl chain is located closely to the metallic core over a bipyridine plane with a restricted conformational mobility. The weak signals detected between 6.9 and 7.5 ppm on one hand, and at 8.73 and 8.78 ppm on the other hand correspond very

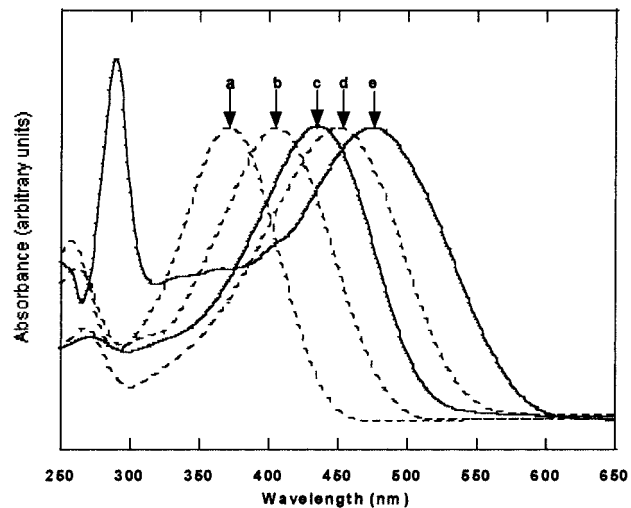


**Figure 5.** UV–Visible spectra of (a) regioregular quater(3-octylthiophene), (b) regioregular sexi(3-octylthiophene), (c) polymer **P4** and (d) regioregular poly(3-octylthiophene) in solution in  $\text{CHCl}_3$ , and (e) polymer **P4–Ru** in solution in  $\text{CH}_3\text{CN}$ .

probably to respectively oligothiophene and bipyridine chain terminations. From their integration ratio, we can estimate the chain length of **P4–Ru** to be of 20 repeating units, which corresponds to  $M_w = 27\,000 \text{ g mol}^{-1}$  for the polycation. This value should be considered only as a rough estimation because the assignment of the considered signals remains uncertain at this time. However, from a qualitative point of view, it clearly appears that the conditions of the Stille coupling reaction are much more efficient for the synthesis of the unmetalated **P4** despite the insolubility of the later in the reaction medium.

**UV–Visible Spectroscopy.** UV–visible spectra were recorded in chloroform for the metal-free compounds and in acetonitrile for **P4–Ru** (Figure 5). Two bands are observed in the UV–visible spectrum of polymer **P4**. The weaker band at 285 nm is characteristic of a  $\pi \rightarrow \pi^*$  transition centered on the 2,2′-bipyridine unit and

(41)  $^1\text{H}$  NMR spectra of 2,2′-bipyridine, 5,5′-dibromo-2,2′-bipyridine, and of the model compound of polymer **P4** that contains one quater(3-octylthiophene) moiety surrounded by two 2,2′-bipyridine units were recorded in conditions similar to those used for polymer **P4** (tetrachloroethane- $d_2$ ,  $70^\circ\text{C}$ ). In these spectra, the signal of  $\text{H}_6$  was located at respectively 8.62, 8.66, and 8.7 ppm. The proton  $\text{H}_a$  of quater(3-octyl)thiophene gave a doublet at 7.1 ppm in the  $^1\text{H}$  NMR spectrum recorded in the same conditions.

the broad and more intense band at 440 nm ( $\epsilon = 33\,500\text{ M}^{-1}\text{ cm}^{-1}$  by monomer unit) corresponds to the  $\pi \rightarrow \pi^*$  transition of the conjugated backbone. The latter band at lower energy is characteristic of the effective conjugation length of the polymer.<sup>42</sup> Its blue shift relative to regioregular POT indicates that incorporation of bipy units into the conjugated backbone lowered the delocalization of  $\pi$  electrons. According to Chen et al.,<sup>43</sup> this effect may be caused by an electronic structural mismatch between adjacent units (i.e., electron-poor bipy and electron-rich quaterthiophene) and/or by structural distortions associated with the presence of bipyridine (i.e., increase of the dihedral angle between pyridine rings and/or between pyridine and thiophene adjacent rings). The blue shift of the absorption peak of **P4** relative to regioregular POT is only 0.05 eV, which implies that  $\pi$  attenuation caused by the alternation of bipy and thiophene oligomers should be of limited magnitude. This is reinforced by the pronounced red shift of the absorption peak of **P4** relative to quater- and sexi-(3-octylthiophene)s (curve a and b, respectively), which demonstrates that  $\pi$  delocalization extends over bipy units. Another explanation to the relatively good electronic delocalization of **P4** compared to POT arises from the regular alternation of electron-rich and electron-poor units in **P4**. This type of structure is known to lead to intramolecular charge transfer within the conjugated framework resulting in the stabilization of the lower band-gap quinoidal-like structure.<sup>44</sup> However, when considering the large electrochemical gap of about 3 eV observed for **P4** (vide infra), such internal charge-transfer phenomenon should be of minor importance in that case. Moreover, any charge-transfer character should decrease the fluorescence yield compared to the homogeneous homopolymer POT, which is not the case.<sup>45</sup> This result is of crucial interest because an efficient delocalization constitutes a necessary condition to provide the polymers (unmetalated and metalated) with good transport properties, and to ensure the connection between the metallic species to be affixed on the bipyridine ligand and the electroactive oligothiophene moieties in the metalated polymers.

The UV-visible spectrum of polymer **P4-Ru** is more complicated. The bipyridine-centered band at 290 nm is more intense than in polymer **P4** because of the presence of two supplementary 2,2'-bipyridines chelating the ruthenium(II) cation in each monomer unit. The shoulders observed around 350 nm correspond to metal-centered transitions<sup>37</sup> and the intense and broad band at 475 nm ( $\epsilon = 56\,500\text{ M}^{-1}\text{ cm}^{-1}$  by monomer unit) is due to the superposition of several transition bands: the  $\pi \rightarrow \pi^*$  transition of the conjugated backbone and the metal to ligands charge transfer (MLCT) transitions involving both the free bipyridines and the polymeric ligand. Indeed, the MLCT transition of  $\text{Ru}(\text{bipy})_3^{2+}$  is observed at 450 nm ( $\epsilon = 14\,500\text{ M}^{-1}\text{ cm}^{-1}$ ) in acetonitrile.

(42) Skotheim, T. A.; Elsenbaumer, R. L.; Reynolds, J. R. *Handbook of conducting polymers*, 2nd ed.; Marcel Dekker: New York, 1998; p 1.

(43) Chen, L. X.; Jäger, W. J. H.; Niemczyk, M. P.; Wasielewski, M. R. *J. Phys. Chem. A*, **1999**, *103*, 4341.

(44) Zhang, Q. T.; Tour, J. M. *J. Am. Chem. Soc.* **1998**, *120*, 5355.

(45) Fluorescence yields of **P4** and of regioregular HT-POT were measured in solution in chloroform and were found to be respectively 0.32 and 0.29 relative to the yield of the coumarin 153 in the same conditions ( $\lambda_{\text{exc}} = 365\text{ nm}$  and  $\text{Abs}_{365} = 0.3$ ).

**Table 3. Redox Potentials of Polymers P4, POT, P4-Ru, and P6-Ru and of the Reference Ru(bipy)<sub>3</sub><sup>2+</sup> Complex**

	$E_{1/2\text{red}}^{\text{V}}$ (vs Ag/Ag <sup>+</sup> )	$E_{1/2\text{ox}}^{\text{V}}$ (vs Ag/Ag <sup>+</sup> )
film of polymer <b>P4</b>	-2.15	0.79; 1.00
film of polymer <b>POT</b>		0.63; 1.15
film of polymer <b>P4-Ru</b>	-2.03; -1.98; -1.61; -1.30	0.65; 0.78; 1.05
film of polymer <b>P6-Ru</b>		0.52; 0.69; 1.07
solution of polymer <b>P4-Ru</b>	-2.14; -2.04; -1.60; -1.34	0.64; 0.78; 1.05
solution of $\text{Ru}(\text{bipy})_3^{2+}$	-2.04; -1.81; -1.63	0.97

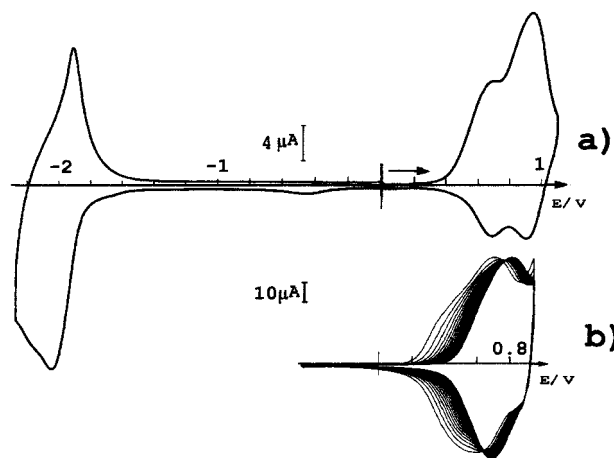


**Figure 6.** Cyclic voltammogram of a film of polymer **P4** cast on a Pt electrode recorded at a scan rate of 20 mV/s in 0.1 M  $[\text{n-Bu}_4\text{N}]\text{PF}_6/\text{CH}_3\text{CN}$ : (a) between 1.2 and -2.2 V and (b) evolution upon cycling.

trile.<sup>37</sup> The band at 475 nm should be dominated by the more intense  $\pi-\pi^*$  transition located on the conjugated backbone ( $\epsilon = 33\,500\text{ M}^{-1}\text{ cm}^{-1}$  by monomer unit in **P4**). Interestingly, the formation of the Ru(II) complex causes a large red shift of 0.21 eV relative to **P4**. On the same basis as that for the discussion above, we postulated that the lowering of the energy of the  $\pi-\pi^*$  transition was mainly due to geometrical factors. The formation of the complex forces the pyridine rings to adopt a syn coplanar geometry,<sup>46</sup> causing an increased  $\pi$ -orbital overlap. In contrast, the structural electronic mismatch between electron-rich thiophene units and even more electron-deficient pyridine rings (due to complexation) should cause a blue shift of that  $\pi-\pi^*$  transition. The geometrical factors seem then to be preponderant in the establishment of an extended delocalization in our polymers. The attribution of the band at 475 nm for **P4-Ru** to the  $\pi-\pi^*$  transition located on the conjugated backbone is confirmed by electrochemical measurements. Indeed, reduction and oxidation processes located on the  $\pi$ -skeleton give an electrochemical gap of 2.03 eV (vide infra) corresponding satisfactorily to the red edge of the  $\pi-\pi^*$  band at 580–600 nm (2.14–2.07 eV).

**Electrochemical Study of Polymers P4 and P4-Ru.** Films of polymer **P4**, cast on a Pt electrode from a chloroform solution, were electrochemically studied between -2 V and +1 V vs Ag/Ag<sup>+</sup> 0.01 M in 0.1 M  $[\text{n-Bu}_4\text{N}]\text{PF}_6/\text{CH}_3\text{CN}$  and in 0.2 M  $[\text{n-Bu}_4\text{N}]\text{PF}_6/\text{CH}_2\text{Cl}_2$  (Table 3, Figure 6a). Two oxidation waves at +0.79 V and +1.00 V were observed both in acetonitrile and dichloromethane. It should be noted that the first

(46) Wang, B.; Wasielewski, M. R. *J. Am. Chem. Soc.* **1997**, *119*, 12.



oxidation wave occurred first at +0.63 V and gradually shifted to its stable value upon cycling without any noticeable loss of electroactivity (Figure 6b), which was assumed to be caused by a reorganization of the film structure. The second wave is not sensitive to this phenomenon and its potential remained constant upon cycling. Comparative coulometric studies were conducted on freshly cast films of **P4** and POT, and electroactivities were determined by integrating the charge passed when applying a voltage 100 mV above the half-wave potential of the studied electrochemical process. It was found that only 0.5 electron per monomer unit (corresponding to four thiophene rings) was released during the first oxidation of **P4** (at 0.73 V), whereas 0.9 electron per quaterthiophene unit were exchanged in the case of POT at 0.73 V. The second oxidation process on **P4** was observed at  $E_{1/2} = +1.00$  V, which is  $\sim 100$  mV lower than for the second oxidation on POT, and corresponds to the additional release of 1.3 electron per monomer unit (to be compared to 0.9 electron per quaterthiophene unit for the second oxidation on POT). The overall electroactivities for **P4** and POT seem then to be comparable since 1.8 electron per quaterthiophene unit were released in both cases, but a strong difference was noticed when considering the first electronic process since only the half of the electroactivity of the POT was recovered in **P4**. This result may be understood if we assume that the electrogenerated oxidized species extends beyond the oligothiophene core, which implies the involvement of the bipyridine  $\pi$ -orbitals in the delocalization process and makes the oxidation of the neighboring monomer unit more difficult. The reduction process occurs at  $E_{1/2} = -2.15$  V, which is very close to the value of  $E_{1/2} = -2.21$  V observed by Yamamoto and co-workers for the  $n$  doping of poly(2,2'-bipyridine),<sup>13</sup> where the electronic overlap between equivalent units is maximized. Compared to polythiophene<sup>47</sup> and to bipyridine ( $E_{1/2} = -2.53$  V in solution in acetonitrile), the reduction of **P4** takes place at a sensibly less negative potential, which indicates that  $\pi$  overlap between oligothiophene and bipyridine cores occurs to some extent, which helps for the stabilization of the electrogenerated reduced species.

**P4–Ru** was studied in the range  $-2.3/+1.5$  V vs Ag/Ag<sup>+</sup>  $10^{-2}$  M both in film cast on a Pt electrode from an acetonitrile solution in 0.4 M  $[n\text{-Bu}_4\text{N}]\text{ClO}_4/\text{CH}_3\text{CN}$  and in solution in 0.1 M  $[n\text{-Bu}_4\text{N}]\text{PF}_6/\text{CH}_3\text{CN}$  (Figure 7, Table 3). Three oxidation waves and four reduction processes were observed in all voltammograms, their position being almost the same for films and solutions of **P4–Ru**. Three well-resolved quasi-reversible oxidation waves were obtained for samples in solution, whereas a drop in electroactivity was observed during the third oxidation wave and the following reduction processes for the films. This is due to a partial dissolution of the polymer films above 1 V. By comparison with the behavior of **P4** in film and  $\text{Ru}(\text{bipy})_3^{2+}$  studied in solution in 0.1 M  $[n\text{-Bu}_4\text{N}]\text{PF}_6/\text{CH}_3\text{CN}$ , we assigned the redox processes as following: (1) the first two oxidation peaks observed at +0.65 V and +0.78 V in films correspond to oxidations on the  $\pi$ -conjugated polymer

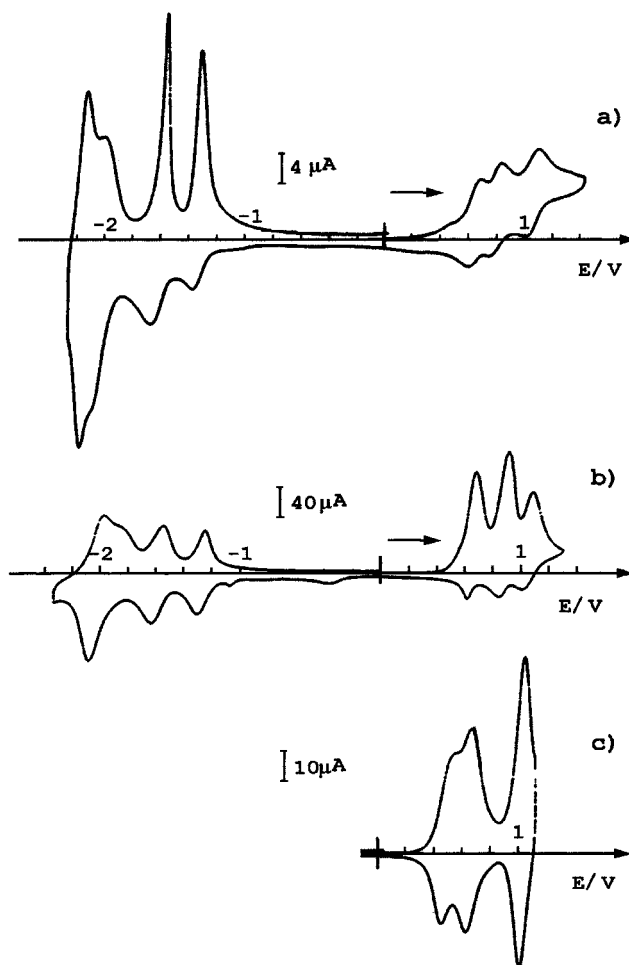


**Figure 7.** Cyclic voltammogram of (a) polymer **P4–Ru** in solution in 0.1 M  $[n\text{-Bu}_4\text{N}]\text{PF}_6/\text{CH}_3\text{CN}$ , (b) polymer **P4–Ru**, and (c) polymer **P6–Ru** in film cast on a Pt electrode in 0.4 M  $[n\text{-Bu}_4\text{N}]\text{ClO}_4/\text{CH}_3\text{CN}$  at a scan rate of 50 mV/s.

backbone. These smaller values compared to polymer **P4** may be explained by the more conjugated structure of **P4–Ru**, as observed by UV–visible spectroscopy, which renders the oxidation processes easier. (2) The third oxidation wave at +1.05 V in solution is centered on the metal. This potential is higher than the one observed for  $\text{Ru}(\text{bipy})_3^{2+}$ , owing to the interaction with the positive charges already introduced on the polymeric chains during the previous oxidation processes. This assignment was confirmed by studying films of polymer **P6–Ru** (the analogue of polymer **P4–Ru** with two additional 3-octylthiophene units) in the same conditions as for films of **P4–Ru**. Three oxidation waves were again obtained: (1) The first two peaks located at 0.52 V and 0.69 V are shifted to low potentials compared to **P4–Ru**. They correspond to oxidations on the  $\pi$ -conjugated backbone and are mainly centered on sexi(3-octylthiophene) moieties which are easier to oxidize than the quater(3-octylthiophene) moieties of polymer **P4–Ru**. (2) The third wave is located at 1.07 V, nearly the same potential as for **P4–Ru**. It is insensitive to the number of thiophene units because it is located on the metal. The reduction behavior of **P4–Ru** is nearly the same for samples in films and solutions. Four reduction waves are observed: the two firsts are well-resolved and the last two are nearly stacked. The unusual sharpness of the two reoxidation waves located at  $-1.3$  V and  $-1.55$  V in the voltammograms obtained from solutions

(47) Sato, M.; Tanaka, S.; Kaeriyama, K. *J. Chem. Soc., Chem. Commun.* **1987**, 1725. Crooks, R. M.; Chyan, O. M. R.; Wrighton, M. S. *Chem. Mater.* **1989**, 1, 2.

of **P4–Ru** are certainly attributable to physical processes accompanying the reduction of polymer **P4–Ru** at the electrode surface. The two corresponding redox processes are quasi-reversible for film samples. The reduction behavior of **P4–Ru** is essentially attributable to the ruthenium complex, with three waves corresponding to the formal redox couples Ru(II)/Ru(I), Ru(I)/Ru(0), and Ru(0)/Ru(–I) at respectively  $-1.34$  V,  $-1.60$  V, and  $-2.04$  V or  $-2.14$  V in solution. Since these electronic processes involve the LUMO of the complex, which is essentially  $\pi^*$  of the ligands in character, the  $E_{1/2}$  values strongly depend on the nature of the ligands. Thus, the first reduction wave, which is observed at sensibly less negative potential than for the reference Ru(bipy) $_3^{2+}$ , is very probably localized on the bipyridine units included in the conjugated polymer, whereas the second and third reduction waves are localized on the remaining unsubstituted ligands. The attribution of the last reduction wave remained unclear until now; it may correspond to a second reduction on the  $\pi$ -conjugated backbone. As the first oxidation and reduction of **P4–Ru** concern the  $\pi$ -conjugated polymer, we can conclude that the metalation of polymer **P4** induces a decrease of the electrochemical gap of the conjugated system. Similar results were obtained with the optical gap of polymer **P4** when the  $\pi$ - $\pi^*$  transition was red-shifted when the conjugated backbone was involved in the complexation of Ru(II).

### Conclusion

Two strategies have been developed to synthesize a novel, structurally defined, all-conjugated polymer in which transition metal complexes are directly affixed onto the conjugated backbone.

The first strategy consisted of the complexation of the presynthesized metal-free polymer. The use of the Stille cross-coupling reaction allowed the preparation of samples of polymer **P4** that exhibited a high degree of polymerization, a high purity and a defect-free conjugated structure. Unfortunately, preliminary experiments that aimed at introducing ruthenium in this structure have failed until now. **P4–Ru** was then obtained following an alternative way that consists of synthesizing first a bis-functionalized metallic core and building the polymeric conjugated backbone in the second step. Because of their solubility in common organic solvents, both polymers were extensively characterized by UV–vis and NMR spectroscopies and by electrochemistry. An extended delocalization of the conjugated backbone was evidenced to take place in both polymers despite the difference in the electronic densities of the constituting units. The complexation of the Ru(II) core affects the electronic properties of the polymer, which was evidenced through the reduction of the optical and electrochemical gaps. Finally, **P4** and **P4–Ru** are the first members of an homogeneous family of polymers, whose chemical structure may be varied in a continuous way, opening a wide field of potential applications such as electroluminescence for nonmetalated polymers (actually under study) and photoconductivity for metalated polymers.

### Experimental Section

**Instrumentation.** Proton NMR spectroscopy was performed at 200 MHz on a Brücker AM-200 spectrometer or at 400 MHz on a Varian U-400 spectrometer, using solvents as

internal references. Chemical shifts ( $\delta$ ) are reported in ppm downfield from tetramethylsilane. UV–visible spectra were recorded on a Perkin-Elmer Lambda 900 spectrometer. HPLC experiments were conducted on a Waters Delta Prep 4000 chromatograph equipped with an absorbance detector tuned at 254 nm. Analyses were performed using two cartridges (Delta-Pak C18, 15  $\mu$ m, 15 Å, 8  $\times$  100 mm or NovaPak C18, 6  $\mu$ m, 60 Å, 8  $\times$  100 mm). Preparative runs were performed using three PrepPak cartridges (Delta-Pak C18, 15  $\mu$ m, 100 Å, 40  $\times$  100 mm). Gel permeation chromatography experiments were performed using Jordi Gel DVB Mixed Bed columns (two columns 10  $\times$  250 mm) calibrated with polystyrene standards. Fast atom bombardment (FAB) mass spectra and accurate-mass spectra were determined on a VG Analytical ZAB–SEQ mass spectrometer. Electrospray mass spectroscopy spectra were performed on a LCQ quadrupole ion trap (Thermoquest) spectrometer. Elemental analyses were carried out by the Service Central d'Analyses, CNRS, B. P. 22, 69390 Vernaison, France, or by the Service de Caractérisation of Institut Charles Sadron, UPR 22, 6 rue Boussingault, 67083 Strasbourg Cedex, France. Light scattering experiments were performed on a FICA 50 spectrometer.

Electrochemical experiments were performed using PAR 173, 175, and 179 units from EG&G Princeton Applied Research connected to a SEFRAM TGM 164 or a KIPP&ZONEN BD 91 recorder in a typical three-electrodes cell containing a Pt working electrode (0.07 cm $^2$ ), a Pt counter electrode and a Ag/Ag $^+$  (AgNO $_3$  10 $^{-2}$  M) nonaqueous reference electrode. Reference electrodes were calibrated by obtaining cyclic voltammograms of a standard ferrocene (Fc) solution.  $E_{1/2}$  for the Fc/Fc $^+$  reversible couple was obtained at 0.10 V. *n*-Bu $_4$ NPF $_6$  was dried under vacuum at 100 °C and stored under argon. The solvents were used without purification, but the solutions were degassed by argon bubbling prior to use.

**Reagents.** All operations were carried out under a dry oxygen-free argon atmosphere. Chemicals were purchased from Aldrich or Acros and used without purification except for DMF, pyridine, and toluene that were distilled respectively over molecular sieves, over KOH, and from P $_2$ O $_5$ . Dry tetrahydrofuran (THF) was distilled under argon from sodium benzophenone ketyl. 2-Bromo-3-octylthiophene, $^{25}$  the chlorinated alkylated quaterthiophene (**4**) (3,4',4'',4'''-tetraoctyl-5'''-chloro-2,2':5',2'':5'',2'''-quaterthiophene), $^{25}$  5,5'-dibromo-2,2'-bipyridine (**1**), $^{34}$  and dichloro-bis-2,2'-bipyridine ruthenium(II) $^{35}$  (Ru(bipy) $_2$ Cl $_2$ ) were synthesized as described in the literature. Pd(PPh $_3$ ) $_3$  $^{48}$  and Pd(PPh $_3$ ) $_2$  $^{39}$  were prepared just before use in carefully degassed anhydrous THF.

**2-Trimethylstannyl-3-octylthiophene (6).** To magnesium turnings (0.20 g, 8.2 mmol) in anhydrous THF (10 mL), heated to maintain a mild reflux, was added dropwise 2-bromo-3-octylthiophene (2.00 g, 7.3 mmol). At the end of the addition, the reaction mixture was refluxed for 2 h before being transferred via cannula to a solution of trimethyltin chloride (1.60 g, 8.0 mmol) in THF (8 mL) at  $-78$  °C. The mixture was allowed to warm to room temperature and stirred overnight before being poured onto water. The aqueous layer was extracted with hexane and the organic extracts were washed with brine and dried over sodium sulfate. The solvent was removed by rotary evaporation to provide 2.48 g of a yellow liquid that contained 93% of 2-trimethylstannyl-3-octylthiophene (yield 87%) and 7% of 3-octylthiophene (determined by  $^1$ H NMR spectroscopy). This product was used without any further purification in the following coupling test reactions.  $^1$ H NMR (CDCl $_3$ , 200 MHz):  $\delta$  7.53 (d,  $J$  = 4.8 Hz, 1 H), 7.09 (d,  $J$  = 4.8 Hz, 1H), 2.62 (t,  $J$  = 7.8 Hz, 2H), 1.55 (m, 2H), 1.28 (m, 10 H), 0.88 (m, 3H), 0.37 (s, 9H). Signals corresponding to 3-octylthiophene were detected at 7.23 (m, 0.07H), 7.93 (m, 0.14H).

**General Procedure for the Coupling Test Reaction: Synthesis of 5,5'-Bis(3-octylthiophene)-2,2'-bipyridine (7).** A solution of 5,5'-dibromo-2,2'-bipyridine (**1**) (0.200 g, 0.64 mmol) and 2-trimethylstannyl-3-octylthiophene (**6**) (0.505 g,

(48) Smith, G. B.; Dezeny, G. C.; Hughes, D. L.; King, A. O.; Verhoeven, T. R. *J. Org. Chem.* **1994**, *59*, 8151.

1.41 mmol, 2.2 equiv) in DMF, pyridine, or toluene (20 mL) was carefully degassed by three freeze–thaw cycles, and the appropriate catalyst ( $3.84 \times 10^{-2}$  mmol, 0.06 equiv) was added. After the mixture was heated at 120, 135, or 110 °C for various times (Table 1), the solvent was removed under vacuum. The product was dissolved in a mixture of diethyl ether (100 mL) and THF (35 mL), and the resulting solution was washed successively with aqueous KF 0.5 M, water, and brine and was dried over sodium sulfate. The solvent was removed by rotary evaporation and the residue was purified by semipreparative HPLC on reverse phase, using a mixture acetonitrile/dichloromethane (75/25) containing 0.01% of triethylamine, yielding **7** as a yellow oil.  $^1\text{H NMR}$  ( $\text{CDCl}_3$ , 200 MHz):  $\delta$  8.78 (dd,  $J = 2.2$  Hz,  $J = 0.6$  Hz, 2H), 8.47 (dd,  $J = 8.3$  Hz,  $J = 0.6$  Hz, 2H), 7.88 (dd,  $J = 8.3$  Hz,  $J = 2.5$  Hz, 2H), 7.33 (d,  $J = 5.1$  Hz, 2H), 7.04 (d,  $J = 5.1$  Hz, 2H), 2.70 (t,  $J = 8.4$  Hz, 4H), 1.59 (m, 4H), 1.24 (m, 20H), 0.86 (m, 6H).  $^{13}\text{C NMR}$  ( $\text{CDCl}_3$ , 200 MHz):  $\delta$  154.98, 149.83, 140.95, 137.92, 134.34, 131.62, 130.53, 125.56, 121.31, 32.54, 31.75, 30.15, 30.06, 29.91, 29.48, 23.33, 14.78. FAB/MS (NBA):  $m/z = 545.2$  ( $\text{MH}^+$ ); calcd for  $\text{C}_{34}\text{H}_{44}\text{N}_2\text{S}_2 = 544.8$ . Anal. Calcd for  $\text{C}_{34}\text{H}_{44}\text{N}_2\text{S}_2$ : C, 74.95; H, 8.14; N, 5.14; S, 11.77. Found: C, 75.13; H, 8.18; N, 5.21; S, 11.56. UV–vis ( $\text{CHCl}_3$ ):  $\lambda_{\text{max}} = 336$  nm.

**Bis(2,2'-bipyridine)(5,5'-dibromo-2,2'-bipyridine)ruthenium(II) Hexafluorophosphate (3).** *cis*-Dichlorobis(2,2'-bipyridine)ruthenium (0.301 g, 0.621 mmol) and 5,5'-dibromo-2,2'-bipyridine (**1**) (0.195 g, 0.621 mmol) were dissolved in ethanol 96%. The mixture was heated at reflux for 24 h. The solution was evaporated to dryness, and the residue was purified by gravity chromatography, using silica gel 60 and a mixture acetonitrile/water/saturated aqueous  $\text{KNO}_3$  (80/19.8/0.2) as eluent. After the acetonitrile was removed by rotary evaporation, excess potassium hexafluorophosphate was added to the solution, enabling the immediate precipitation of **3**. The filtration of the aqueous solution provided 0.575 g (91%) of **3** as a red solid.  $^1\text{H NMR}$  ( $\text{DMSO}-d_6$ , 400 MHz, 343 K):  $\delta$  8.78 (d,  $J = 8.0$  Hz, 4H), 8.74 (d,  $J = 8.4$  Hz, 2H), 8.42 (dd,  $J = 8.4$  Hz,  $J = 2.0$  Hz, 2H), 8.18 (td,  $J = 8.0$  Hz,  $J = 1.6$  Hz, 2H), 8.16 (td,  $J = 8.0$  Hz,  $J = 1.6$  Hz, 2H), 7.85 (d,  $J = 5.6$  Hz, 2H), 7.69 (d,  $J = 5.6$  Hz, 2H), 7.67 (d,  $J = 2.0$  Hz, 2H), 7.53 (m, 4H). ESMS  $m/z = 872.8$  ( $\text{M-PF}_6$ ); Calcd for  $\text{C}_{30}\text{H}_{22}\text{N}_6\text{Br}_2\text{RuPF}_6$ : 872.4. UV–vis ( $\text{CH}_3\text{CN}$ ):  $\lambda_{\text{max}} = 287, 449$  nm.

**Procedure for the Coupling Test Reaction with the Metalated 2,2-Bipyridine Moiety: Synthesis of 9.** A solution of **3** (0.150 g, 0.147 mmol) and 2-trimethylstannyl-3-octylthiophene (**6**) (0.116 g, 0.323 mmol, 2.2 equiv) in DMF (5 mL) was carefully degassed by three freeze–thaw cycles. Freshly prepared  $\text{Pd}(\text{PPh}_3)_2$  (0.06 equiv,  $8.82 \times 10^{-3}$  mmol) was added, and the mixture was stirred at 120 °C overnight. The solvent was then removed under vacuum and the residue was purified by gravity chromatography on silica gel eluted with acetonitrile/water/saturated aqueous  $\text{KNO}_3$  (90.5/9.4/0.1). After removal of acetonitrile by rotary evaporation, **9** was precipitated by the addition of potassium hexafluorophosphate, giving 180 mg (98%) of a red solid.  $^1\text{H NMR}$  ( $\text{DMSO}-d_6$ , 400 MHz, 343 K):  $\delta$  8.89 (m, 6H), 8.18 (m, 6H), 7.97 (d,  $J = 5.6$  Hz, 2H), 7.80 (d,  $J = 5.6$  Hz, 2H), 7.69 (s, 2H), 7.62 (d, 5.6 Hz, 2H), 7.55 (m, 4H), 7.03 (d,  $J = 5.2$  Hz, 2H), 2.31 (m, 2H), 2.16 (m, 2H), 1.32 (m, 24H), 0.83 (m, 6H). ESMS  $m/z = 1103.0$  ( $\text{M-PF}_6$ ). Calcd for  $\text{C}_{59}\text{H}_{60}\text{N}_6\text{S}_2\text{RuPF}_6$ : 1103.28. UV–vis ( $\text{CH}_3\text{CN}$ ):  $\lambda_{\text{max}} = 259, 291, 330, 373, 459$  nm.

**3,4',4'',4'''-Tetraoctyl-2,2':5',2'':5''',2''''-quaterthiophene (5): Dechlorination reaction.** A mixture containing the chlorinated oligomer **4** (0.50 g, 0.61 mmol), an excess of tributyltin hydride (4 equiv), and 5 mg of AIBN in 4 mL of anhydrous THF was refluxed overnight before being poured onto water. The aqueous phase was extracted with hexane, and the organic extracts were washed with aqueous KF 0.5 M, water and brine and dried over sodium sulfate. The solvent was removed by rotary evaporation, and the residue was treated with an excess of *p*-toluenesulfonic acid in 40 mL of refluxing THF overnight. The mixture was then poured onto water, and the aqueous phase was extracted with hexane. The organic extracts were washed with aqueous  $\text{NaHCO}_3$ , water, and brine and dried over sodium sulfate. The solvent was

removed by rotary evaporation, and the residue was purified by semipreparative HPLC on reverse phase, using a dichloromethane/acetonitrile (47/53) as eluent, giving 0.44 g of **5** (92%).  $^1\text{H NMR}$  ( $\text{C}_2\text{D}_2\text{Cl}_4$ , 400 MHz, 343 K):  $\delta$  7.10 (d,  $J = 5.2$  Hz, 1H), 6.89 (m, 5H), 2.72 (m, 6H), 2.57 (m, 2H), 1.61 (m, 8H), 1.24 (bs, 40H), 0.84 (m, 12H). HRMS Calcd for  $\text{C}_{48}\text{H}_{74}\text{S}_4$ : 778.4675. Found: 778.4693. Anal. Calcd for  $\text{C}_{48}\text{H}_{74}\text{S}_4$ : C, 73.98; H, 9.57. Found: C, 73.98; H, 9.57.

**3,4',4'',4'''-Tetraoctyl-5,5''-bis(trimethylstannyl)-2,2':5',2'':5''',2''''-quaterthiophene (2).** To a solution of free-ends quater(3-octylthiophene) **5** (0.400 g, 0.513 mmol) in 20 mL of anhydrous THF at  $-78$  °C was added dropwise a 2.5 M solution of *n*-BuLi in hexane (1.283 mmol, 2.5 equiv). The mixture was allowed to warm to room temperature and stirred for 1 h before being cooled again to  $-78$  °C. A solution of trimethyltin chloride (1.283 mmol, 2.5 equiv) in 4 mL of anhydrous THF was added to the reaction mixture that was then brought again to room temperature and stirred for a further hour before being poured onto water. The aqueous layer was extracted with hexane and the organic extracts were washed rapidly with brine before being dried over sodium sulfate. The solvent was removed by rotary evaporation, and the residue was purified by semipreparative HPLC on reverse phase eluted with a mixture amylene-stabilized dichloromethane/acetonitrile (52/48) containing 0.02% of triethylamine, to provide 556 mg (98%) of **2**.  $^1\text{H NMR}$  ( $\text{CD}_2\text{Cl}_2$ , 200 MHz):  $\delta$  7.10 (s, 1H), 6.99 (s, 1H), 6.94 (s, 1H), 6.92 (s, 1H), 2.75 (m, 6H), 2.58 (m, 2H), 1.62 (m, 8H), 1.26 (bs, 40 H), 0.85 (m, 12 H), 0.38 (s, 9H), 0.35 (s, 9H). ESMS  $m/z = 1104.3$  (M); calcd for  $\text{C}_{54}\text{H}_{90}\text{S}_4\text{Sn}_2$ : 1104.9.

**Polymer P4.** A solution of **2** (0.181 g, 0.164 mmol) and 5,5'-dibromo-2,2'-bipyridine (**1**) (0.051 g, 0.164 mmol) in DMF (11 mL) was carefully degassed by four freeze–thaw cycles, and freshly prepared  $\text{Pd}(\text{PPh}_3)_2$  (0.06 equiv,  $9.84 \times 10^{-3}$  mmol) was added. After the mixture was stirred at 120 °C for 24 h, the solid formed was separated from the reaction medium and extracted in a Soxhlet apparatus successively with ethanol, hexane, 1,2-dimethoxyethane (to remove inorganic impurities and short oligomers), and finally with chloroform. Evaporation to dryness of the chloroform extract gave 84 mg (55%) of **P4** as a dark red solid. A total of 10 mg (6.5%) of an insoluble dark red solid was recovered in the cartridge.  $^1\text{H NMR}$  ( $\text{C}_2\text{D}_2\text{Cl}_2$ , 400 MHz, 343 K):  $\delta$  8.94 (m, 1H), 8.82 (m, 1H), 8.54 (m, 2H), 8.03 (m, 1H), 7.96 (m, 1H), 7.29 (s, 1H), 7.06 (s, 1H), 7.01 (s, 1H), 6.98 (s, 1H), 2.92 (m, 8H), 1.68 (m, 8H), 1.25 (m, 40H), 0.84 (m, 12 H). Anal. Calcd for  $\text{C}_{58}\text{H}_{78}\text{S}_4\text{N}_2$ : C, 74.78; H, 8.44; S, 13.77; N, 3.01. Found: C, 73.50; H, 8.38; S, 13.59; N, 2.84.

**Polymer P4–Ru.** A solution of **2** (0.261 g, 0.236 mmol) and **3** (0.240 g, 0.236 mmol) in DMF (17 mL) was carefully degassed by four freeze–thaw cycles. Freshly prepared  $\text{Pd}(\text{PPh}_3)_2$  (0.06 equiv,  $1.42 \times 10^{-2}$  mmol) was added, and the mixture was stirred at 120 °C for 24 h. The solvent was evaporated under vacuum until 1–2 mL was left, and water (100 mL) was added. The resulting precipitate was filtered and thoroughly washed with methanol, before being extracted in a Soxhlet apparatus successively with methanol and ethanol to give respectively 61 mg (16%) and 10 mg (3%) of soluble low molecular weight polymer. The insoluble part was collected, dissolved in the minimum amount of acetonitrile, and partitioned by precipitation upon addition of water to give 196 mg (51%) of **P4–Ru** as a red solid. A total of 81 mg (21%) of polymer was left in the filtrate.  $^1\text{H NMR}$  ( $\text{DMSO}-d_6$ , 400 MHz, 343 K):  $\delta$  8.85 (m, 6H), 8.40 (m, 1H), 8.21 (m, 5H), 7.99 (m, 2H), 7.90 (m, 1H), 7.81 (m, 2H), 7.60 (m, 5H), 7.40 (s, 1H), 7.15 (s, 1H), 7.12 (2, 1H), 7.09 (s, 1H), 2.78 (m, 6H), 2.31 (m, 1H), 2.16 (m, 1H), 1.63 (m, 6H), 1.24 (m, 42H), 0.83 (m, 12H).

**Acknowledgment.** The authors thank C. Lebrun (DRFMC/SCIB/RI, CEA/Grenoble) for mass spectrometry measurements and F. Sarrazin (DRFMC/SCIB/LAN), for  $^1\text{H NMR}$  experiments. We are very grateful to M. Mottin, who performed the light scattering experiments.

CM990807U